MECHANIKA TEORETYCZNA
I STOSOWANA
Journal of Theoretical
and Applied Mechanics
3, 31, 1993

ACTIVE VIBRATION CONTROL OF ONE-DIMENSIONAL PIEZOELECTRIC LAMINATES

MAREK PIETRZAKOWSKI

Institute of Machine Designe Fundamentals

Warsaw University of Technology

In the paper a theoretical model of a simply supported three-layer one-dimensional plate with a distributed actuator/sensor pair has been examined. A velocity feedback control is used to achieve active damping of structure. The transfer functions relating the out-of-plane deformation to the actuator voltage input for the system without control loop and for the system with velocity feedback as well as the open-loop transfer function are obtained. The numerical results show the influence of the actuator/sensor location and controler parameters on the modal system response.

1. Introduction

The application of piezoelectric actuators and sensors to the active vibration control of flexible structures has been investigated by many authors. Some of them concentrated on static and dynamic response of beams or plates due to an excitation of piezoelectric actuators bonded to the surface or embedded into the structure (cf Crawley and Luis, 1987; Clarc et al., 1991; Pan et al., 1991; Wang and Rogers, 1991). The sensing ability of piezoelectric elements was applied by the others to develop the effect of active damping. The structures with actuator/sensor pairs and the velocity feedback control have been studied by Newman (1991), Alberts and Colvin (1991) (beams) and Lee et al. (1991) (one-dimensional plates). The static approach is commonly used to describe the mechnical coupling between the actuator and the structure. The static model for one-dimensional piezoelectric elements has been developed by Crawley and Luis (1987) and applied by Clarc et al. (1991), Newman (1991), Alberts and Colvin (1991) among others. However, another idea for modelling the interaction between the actuator and the structure has been proposed by Pan et al. (1991) (dynamic model) and by Wang and Rogers (1991) (strain-energy model).

In the paper a theoretical model of a simply supported one-dimensional laminated plate with piezoelectric layers has been examined. Basing on the static strain/stress analysis, two concepts of determining the equivalent bending moment caused by the actuator are compared. The velocity feedback control is used to achieve the active damping of structure. The system response is obtained applying the laminated beam theory (Whitney, 1987). The transfer functions relating the out-of-plane deformation under the actuator voltage input for the system without the control loop and for the system with velocity feedback as well as the open-loop transfer function, respectively, are obtained. The numerical results show the influence of the actuator/sensor location and control parameters on the modal system response.

2. Model of one-dimensional piezoelectric laminate

The system investigated in this article is a three-layer rectangular composite plate simply supported at the opposite edges as shown in Fig.1. The plate is composed of a stainless steel shim with piezoelectric layers bonded to the upper and lower surfaces, respectively. The piezoelectric layers are made of PZTG-1195 film. Because of the piezoelectric properties, the material isotropy is assumed (cf Crawley and Luis, 1987). The upper lamina acts as the actuator while the lower layer is used as the sensor. Only the portion of the piezoelectric layer covered by an electrode on both sides of the layer is activated. The identical, symmetrically located rectangular surface electrodes attached to actuator and sensor layers, respectively, are used in the considered structure.

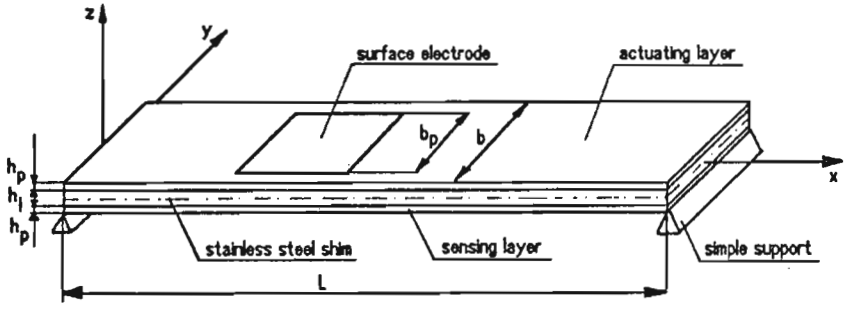

Fig. 1. A simply supported beam with a sensor/actuator pair

According to the clasical laminate plate theory, the Kirchhoff hypothesis is accepted. Hence, for thin plates, a plane stress state exists. The equation of motion for out-of-plane displacements, $w(x, y, t)$, of a plate composed of isotropic

layers can be written as

$$D_{11}\left(\frac{\partial^4 w}{\partial x^4}+2\frac{\partial^4 w}{\partial x^2\partial y^2}+\frac{\partial^4 w}{\partial y^4}\right)+\rho h\frac{\partial^2 w}{\partial t^2}=g(x,y,t) \tag{2.1}$$

where $g(x,y,t)$ represents an external load; $h=2h_p+h_l$ is the thickness of laminate; ρ is the equivalent density of laminate which in the considered case becomes

$$\rho=\frac{1}{h}(2\rho_p h_p+\rho_l h_l) \tag{2.2}$$

The subscripts l and p indicate the shim metal layer and the piezoelectric ply, respectively.

The flexural rigidity of the plate is given by

$$D_{11}=\frac{E_l}{1-\nu_l^2}\left(\frac{h_l^3}{12}\right)+\frac{E_p}{1-\nu_p^2}h_p\left(\frac{1}{2}h_l^2+h_l h_p+\frac{2}{3}h_p^2\right) \tag{2.3}$$

where E, ν represents the Young modulus and the Poisson ratio of the layer, respectively.

Assuming that the length is much greater than the width of the plate, i.e., $L \gg b$, and the intensity of a load g does not change in y direction, displacements w may be considered to be independent of the width coordinate (y axis). Therefore, the equation of motion of a one-dimentional plate is obtained

$$D_{11}\frac{\partial^4 w}{\partial x^4}+\rho h\frac{\partial^2 w}{\partial t^2}=g(x,t) \tag{2.4}$$

Since, the isotropic plies of the laminate are oriented symmetrically about the midplane, the deflection of the plate can be analysed in terms of the classical beam theory replacing the bending stiffness EJ by the equivalent stiffness E^bJ defined as follows, (see Whitney, 1987)

$$E^bJ=\sum_{k=1}^{N}E^kJ^k \tag{2.5}$$

where E^b is the effective bending modulus of the laminated beam; E^k is the modulus of the kth layer; J and J^k is the moment of inertia of the beam and the moment of inertia of kth layer relative to the midplane, respectively.

Applying laminated beam theory (Whitney, 1987), Eq (2.4) describing the motion of the one-dimentional plate can be replaced by the following equation

$$E^bJ\frac{\partial^4 w}{\partial x^4}+\rho A\frac{\partial^2 w}{\partial t^2}=p(x,t) \tag{2.6}$$

where

$$E^b = \frac{12}{h^3} D_{11} \qquad J = \frac{bh^3}{12} \qquad A = bh \qquad p(x,t) = bg(x,t)$$

In the next sections of the article the one-dimentional plate is investigated using the mathematical model of the laminated beam.

3. Actuator relations

In effect of applying a voltage to an unconstrained actuating layer along its polarization direction a strain is induced

$$\varepsilon_a = \frac{d_{31}}{h_p} V_a \tag{3.1}$$

that is a function of the piezoelectric strain constant d_{31}, the applied voltage V_a, and the element thickness h_p, respectively.

In the simplified model of the system, the piezoelectric layers are perfectly bonded to the metal shim with zero glue thickness. Because the layers are narrow with respect to their length, only the bending effect is considered. Extension of the actuator produces the longitudinal interface strains in the x direction and a bending moment about the neutral axis of the laminated beam.

In the paper two concepts of determining the equivalent bending moment based on the static strain/stress analysis are used.

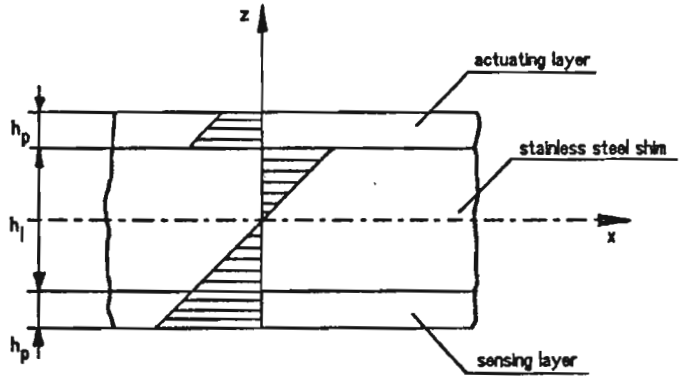

Fig. 2. Stress distribution

The first concept is presented by Crawley and Luis (1987), Clarc et al. (1991). In the considered structure it is assumed that the effective piezoelectric patch induces the linear stress distribution which is shown in Fig.2.

The shim and actuator interface stresses σ_l^i depend on the interface strains ε^i according to Hook's law

$$\sigma_l^i = E_l \varepsilon^i \tag{3.2}$$

where the upper script i is used to designate the interface.

The actuator stresses σ_a^i at the interface are the result of the metal shim strains and the unconstrained actuator strains, respectively

$$\sigma_a^i = E_p(\varepsilon^i - \varepsilon_a) \tag{3.3}$$

The linear distribution of the normal stresses in the shim and actuator leads to the expressions

$$\sigma_l = 2\sigma_l^i \frac{z}{h_l} \tag{3.4}$$

and

$$\sigma_a = \sigma_a^i - \sigma_l^i\left(1 - 2\frac{z}{h_l}\right) \tag{3.5}$$

Because of the thinness of the piezoelectric layer, the stresses in the sensor are assumed to be distributed according to Eq (3.4). The moment equilibrum about neutral bending axis gives

$$\int_{-\frac{h_l}{2}-h_p}^{\frac{h_l}{2}} \sigma_l z dz + \int_{\frac{h_l}{2}}^{\frac{h_l}{2}+h_p} \sigma_a z dz = 0 \tag{3.6}$$

Substituting Eqs (3.4) and (3.5) into Eq (3.6), after integration, yields the following interface stress

$$\sigma_l^i = -K\sigma_a^i \tag{3.7}$$

where K is a nondimensional parameter specified as

$$K = \frac{3h_l h_p(h_l + h_p)}{h_l^3 + 9h_l h_p^2 + 3h_l^2 h_p + 8h_p^3} \tag{3.8}$$

The interface strain relation can be obtained substituting Eqs (3.2) and (3.3) into Eq (3.7)

$$\varepsilon^i = \frac{KE_p}{E_l + KE_p}\varepsilon_a \tag{3.9}$$

The bending curvature of the interface is the strain function

$$\frac{1}{r^i} = -\frac{2\varepsilon^i}{h_l} \tag{3.10}$$

so the bending moment produced by the actuator can be written as

$$M_a = \frac{2E^bJ}{h_l}\varepsilon^i \tag{3.11}$$

where E^bJ is the eqivalent stiffness of the laminated beam determined by Eq (2.5).

Substituting Eqs (3.9) and (3.1) into Eq (3.11), the relation between the voltage applied to the actuator and the induced bending moment is obtained

$$M_a = C_a V_a \tag{3.12}$$

where the constant C_a depends on the geometry and material properties of the system

$$C_a = \frac{2KE_pE^bJd_{31}}{h_lh_p(E_l + KE_p)} \tag{3.13}$$

The voltage applied to the actuator electrode can be written as a function of separated variables

$$V_a(x,t) = V(t)\Lambda_a(x) \tag{3.14}$$

where $V(t)$ describes the time dependent voltage and $\Lambda_a(x)$ is a spatialy dependent term which informs about the electrode pattern.

The second way of determining the bending moment produced by the actuator is mentioned by Newman (1991), Alberts and Colvin (1991). Because of the small thickness of piezoelectric layer, the normal stresses σ_a are assumed to be uniform in the z direction. For the actuator/sensor layers characterized by the same dimensions and elastic moduli, the force equation along x axis caused by the tension effect of the actuator gives the following strain relation

$$\varepsilon = \frac{E_ph_p}{2E_ph_p + E_lh_l}\varepsilon_a \tag{3.15}$$

where ε is the longitudinal strain of the laminated beam.

The bending moment is calculated from the moment equilibrum of the resultant forces in the actuator and sensor layers about the neutral axis

$$M_a = E_ph_pb_p(\varepsilon_a - 2\varepsilon)\frac{h_p + h_l}{2} \tag{3.16}$$

where b_p is the width of the actuator layer which is activated.

Substituting Eqs (3.15) and (3.1) into Eq (3.16), the bending moment can be expressed by Eq (3.12), where the constant C_a is specified as

$$C_a = \frac{E_lE_pd_{31}(h_l^2 + h_lh_p)b_p}{2(E_lh_l + 2E_ph_p)} \tag{3.17}$$

In the both cases it is assumed that the surface electrode is large compared to the piezoelectric layer thickness, so the produced moments caused by the normal stress distribution create the pure bending of the structure.

4. Sensor relations

The piezoelectric element response on the applied strain ε_s is the charge density on its surface

$$q = \left(\frac{k_{31}^2}{g_{31}}\right)\varepsilon_s \tag{4.1}$$

where k_{31} is the piezoelectric electromechanical coupling constant and g_{31} is the piezoelectric stress constant, (cf Alberts and Colvin, 1991).

The strain ε_s is related to the curvature of the laminated beam and can be expressed by

$$\varepsilon_s = -\left(\frac{h_l + h_p}{2}\right)\frac{\partial^2 w}{\partial x^2} \tag{4.2}$$

When the sensor electrode pattern is determined, the total charge induced on the electrode surface is the integral over the length of the beam

$$Q = \int_0^L q\Lambda_s(x)dx \tag{4.3}$$

where $\Lambda_s(x)$ is the spatial distribution function.

Substituting Eqs (4.1) and (4.2) into Eq (4.3) gives

$$Q = -\left(\frac{k_{31}^2}{g_{31}}\right)\left(\frac{h_l + h_p}{2}\right)\int_0^L \frac{\partial^2 w}{\partial x^2}\Lambda_s(x)dx \tag{4.4}$$

The voltage developed by the sensor is the ratio of the charge and the capacitance, so it is obtained

$$V_s = -C_s\int_0^L \frac{\partial^2 w}{\partial x^2}\Lambda_s(x)dx \tag{4.5}$$

The sensor constant C_s depends on piezoelectric material properties and geometrical parameters characterizing the structure

$$C_s = \left(\frac{k_{31}^2}{g_{31}}\right)\frac{h_l + h_p}{2A_sC_o} \tag{4.6}$$

where A_s is the sensor electrode area and C_o is the capacitance of the area unit.

5. Vibrations of a simply supported one-dimensional piezoelectric laminate

As mentioned earlier, the problem of vibrations of one-dimensional composite plate is solved using laminated beam theory. Assuming external viscous damping

and applying the moment produced by actuator, the equation of motion of the considered system, Eq (2.6), can be rewritten as follows

$$\frac{\partial^2}{\partial x^2}\left[E^b J\frac{\partial^2 w}{\partial x^2} - M_a\right] + \rho A\frac{\partial^2 w}{\partial t^2} + 2\beta\rho A\frac{\partial w}{\partial t} = 0 \tag{5.1}$$

where β is the damping factor.

The term for damping serves a finite response at resonance. The moment M_a replaced by Eq (3.12) and transferred to the right-hand side of Eq (5.1) represents the external load

$$E^b J\frac{\partial^4 w}{\partial x^4} + \rho A\frac{\partial^2 w}{\partial t^2} + 2\beta\rho A\frac{\partial w}{\partial t} = C_a\frac{\partial^2 V_a}{\partial x^2} \tag{5.2}$$

The voltage V_a is a function of time and geometry of the actuator. For the rectangular surface electrode which location is indicated by coordinates x_1 and x_2 and the width is smaller than the width of the laminate, the voltage is given by the equation

$$V_a(x,t) = V(t)\frac{b_p}{b}[H(x-x_1) - H(x-x_2)] \tag{5.3}$$

where $H(x)$ is the unit-step function.

Substituting Eq (5.3) into Eq (5.2), and after differentiating, the following form of the equation of motion can be obtained

$$E^b J\frac{\partial^4 w}{\partial x^4} + \rho A\frac{\partial^2 w}{\partial t^2} + 2\beta\rho A\frac{\partial w}{\partial t} = C_a V(t)\frac{b_p}{b}[\delta'(x-x_1) - \delta'(x-x_2)] \tag{5.4}$$

where $\delta(x)$ is the Dirac delta-function and $\delta'(x) = \partial\delta(x)/\partial x$.

The right-hand side of the above equation represents the external resultant moments acting at boundaries of the actuator surface electrode. The solution to the equation of motion according to the modal analysis can be decomposed into the modal summation

$$w(x,t) = \sum_{n=1}^{\infty} A_n(t)\Phi_n(x) \tag{5.5}$$

where $A_n(t)$ and Φ_n are the modal coordinate and mode shape of the nth vibration mode, respectively.

The mode shape $\Phi_n(x)$ for the simply supported beam has the well-known form

$$\Phi_n(x) = \sin k_n x \tag{5.6}$$

where $k_n = n\pi/L$ is the eigenvalue for the boundary conditions mentioned above.

The mode shape function satisfies the following differential equation

$$\frac{d^4\Phi_n(x)}{dx^4} = k_n^4\Phi_n(x) \tag{5.7}$$

The external load can be rewtitten using the modal summation

$$C_a V(t)\frac{b_p}{b}[\delta'(x-x_1)-\delta'(x-x_2)] = \sum_{n=1}^{\infty} Q_n(t)\Phi_n(x) \tag{5.8}$$

After applying the orthogonality condition, the modal coordinate $Q_n(t)$ becomes

$$Q_n(t) = \frac{2n\pi b_p C_a}{L^2 b}\left[\cos\left(\frac{n\pi x_1}{L}\right) - \cos\left(\frac{n\pi x_2}{L}\right)\right]V(t) \tag{5.9}$$

Considering a harmonic voltage input, $V(t) = e^{j\omega t}$, the modal coordinate $A_n(t)$ of transverse displacements can be obtained by substituting Eqs (5.5), (5.6), (5.8) and (5.9) into the equation of motion (5.2)

$$A_n(t) = \frac{2n\pi b_p C_a}{\rho A L^2 b(\omega_n^2 - \omega^2 + j2\beta\omega)}\left[\cos\left(\frac{n\pi x_1}{L}\right) - \cos\left(\frac{n\pi x_2}{L}\right)\right]e^{j\omega t} \tag{5.10}$$

where the nth resonance frequency ω_n is determined by

$$\omega_n = \left(\frac{n\pi}{L}\right)^2\sqrt{\frac{E_l J}{\rho A}} \tag{5.11}$$

The deflection of the one-dimensional piezoelectric laminate is written directly from Eqs (5.5), (5.6) and (5.10)

$$w(x,t) = \frac{2\pi b_p C_a}{\rho A L^2 b}e^{j\omega t}\cdot$$
$$\cdot\sum_{n=1}^{\infty}\frac{n}{\omega_n^2 - \omega^2 + j2\beta\omega}\left[\cos\left(\frac{n\pi x_1}{L}\right) - \cos\left(\frac{n\pi x_2}{L}\right)\right]\sin\left(\frac{n\pi x}{L}\right) \tag{5.12}$$

The system response can be expressed in terms of the transfer function. The transfer function relating the out-of plane deformation to the actuator voltage input has the form

$$G(x,\omega) = \frac{w(x,\omega)}{V(\omega)} =$$
$$= \frac{2\pi b_p C_a}{\rho A L^2 b}\sum_{n=1}^{\infty}\frac{n}{\omega_n^2 - \omega^2 + j2\beta\omega}\left[\cos\left(\frac{n\pi x_1}{L}\right) - \cos\left(\frac{n\pi x_2}{L}\right)\right]\sin\left(\frac{n\pi x}{L}\right) \tag{5.13}$$

6. Transfer functions of the system with feedback control

The control loop scheme shown in Fig.3 is used to achieve active damping of the vibrations of the structure.

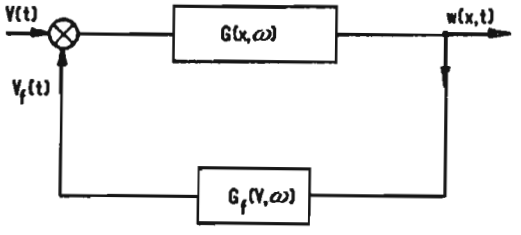

Fig. 3. Scheme of the feedback control loop

The velocity feedback is characterized by the transfer function G_f which represents the ratio of the output voltage signal $V_f(t)$ to the deflection of the laminated beam. The output signal $V_f(t)$ is proportional to the time derivative of the sensor voltage signal, therefore, is proportional to the velocity of the curvature change. Since, the sensing layer is covered by the rectangular electrode extended partially across the width of the lamina, the spatial distribution function $\Lambda_s(x)$ is given by

$$\Lambda_s(x) = b_p[H(x - x_1) - H(x - x_2)] \tag{6.1}$$

The transfer function between the sensor output voltage $V_s(t)$ and the external input actuator voltage $V(t)$ can be obtained from Eqs (4.5), (5.13) and (6.1)

$$G_s(\omega) = -\frac{V_s(\omega)}{V(\omega)} = \\ = \frac{2\pi^2 b_p^2 C_a C_s}{\rho A L^3 b} \sum_{n=1}^{\infty} \frac{n^2}{\omega_n^2 - \omega^2 + j2\beta\omega} \left[\cos\left(\frac{n\pi x_1}{L}\right) - \cos\left(\frac{n\pi x_2}{L}\right)\right]^2 \tag{6.2}$$

Because of the velocity feedback the open-loop transfer function is a product of the transfer function G_s given by Eq (6.2) and the transfer function characterised the differentiating element

$$G_o(\omega) = \frac{V_f(\omega)}{V(\omega)} = G_s(\omega)\frac{jT_d\omega}{1 + jT\omega} \tag{6.3}$$

where T_d and T are the gain constant and the time-lag constant of the differentiator, respectively.

The closed-loop transfer function, which relates the deflection of the beam with the feedback loop to the actuator voltage, can be determined by the well-known equation

$$G_c(x,\omega) = \frac{G(x,\omega)}{1 + G_o(\omega)} \tag{6.4}$$

In the models of real systems damping is often described by the uniform modal damping. The transfer functions G, G_s, G_o, G_c for this kind of damping can be obtained from Eqs (5.13), (6.2), (6.3) and (6.4) substituting

$$\beta = \gamma\omega_n \tag{6.5}$$

where γ is a nondimensional damping factor identical for all modes.

7. Results

To demonstrate the effect of excitation and active damping using piezoelectric elements, the numerical test was carried out. The dimensions and material properties of the simply supported laminated beam and parameters of the piezoelectric G-1195 layers are listed in Table 1, (The main data was taken from Crawley and Luis (1987), Clarc et al. (1991)).

Table 1. Dimensions and properties of the system used in calculation

L	0.38 [m]	$x_2 - x_1$	0.038 [m]
b	0.04 [m]	b_p	0.04 [m]
h_l	0.002 [m]	h_p	0.002 [m]
ρ_l	7800 [kg/m^3]	ρ_p	7275 [kg/m^3]
E_l	2.1×10^{11} [N/m^2]	E_p	6.3×10^{10} [N/m^2]
ν_l	0.33	ν_p	0.28
γ	0.01	d_{31}	$1,9 \times 10^{-10}$ [m/V]

The beam response depends on the location of the actuator/sensor surface electrode in relation to the modal lines for the considered boundary conditions. As an example, the frequency functions of the system for the rectangular electrode located at the center of the beam ($x_1 = 0.171$ m, $x_2 = 0.209$ m) and near to the left support ($x_1 = 0.081$ m, $x_2 = 0.119$ m) are presented in Fig.4 and Fig.5, respectively. In the both cases frequency response functions are calculated at $x = 0.15$ m. The feedback control loop is characterized by the product of the sensor constant and the gain constant $C_s T_d = 1000$ Vs/m. The time-lag of the differentiator is neglected, i.e., $T = 0.0$ s. The actuator constant C_a is obtained according to Eq (3.13) assuming the linear distribution of the normal stresses in the piezoelectric layer.

When the piezoelectric activated part is located symmetrically at the center of the beam, the frequency response of the structure to a harmonic input voltage defined by Eq (5.13) is shown in Fig.4a. There are five modes appearing between $1 \div 3500$ Hz. In this case the actuator works effectively only for modes which refer to the odd resonance frequencies of the system, i.e, $\omega_1 = 38.2$ Hz, $\omega_3 = 344$

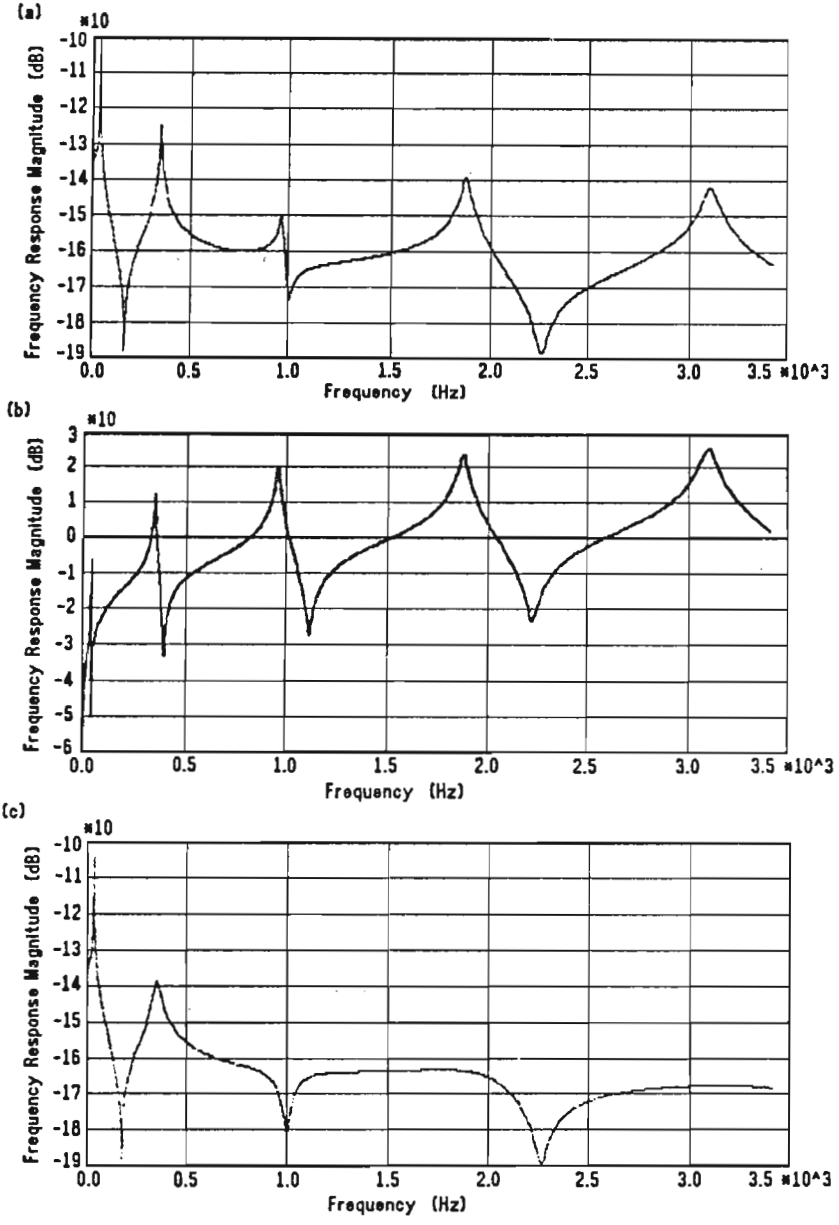

Fig. 4. Frequency response functions for the actuator/sensor location between $x_1 = 0.171$ m and $x_2 = 0.209$ m; (a) magnitude of transfer function G (deflection to voltage input) at $x = 0.15$ m, (b) magnitude of open-loop transfer function G_o (voltage output to voltage input), (c) magnitude of closed-loop transfer function G_c (deflection to voltage input) at $x = 0.15$ m

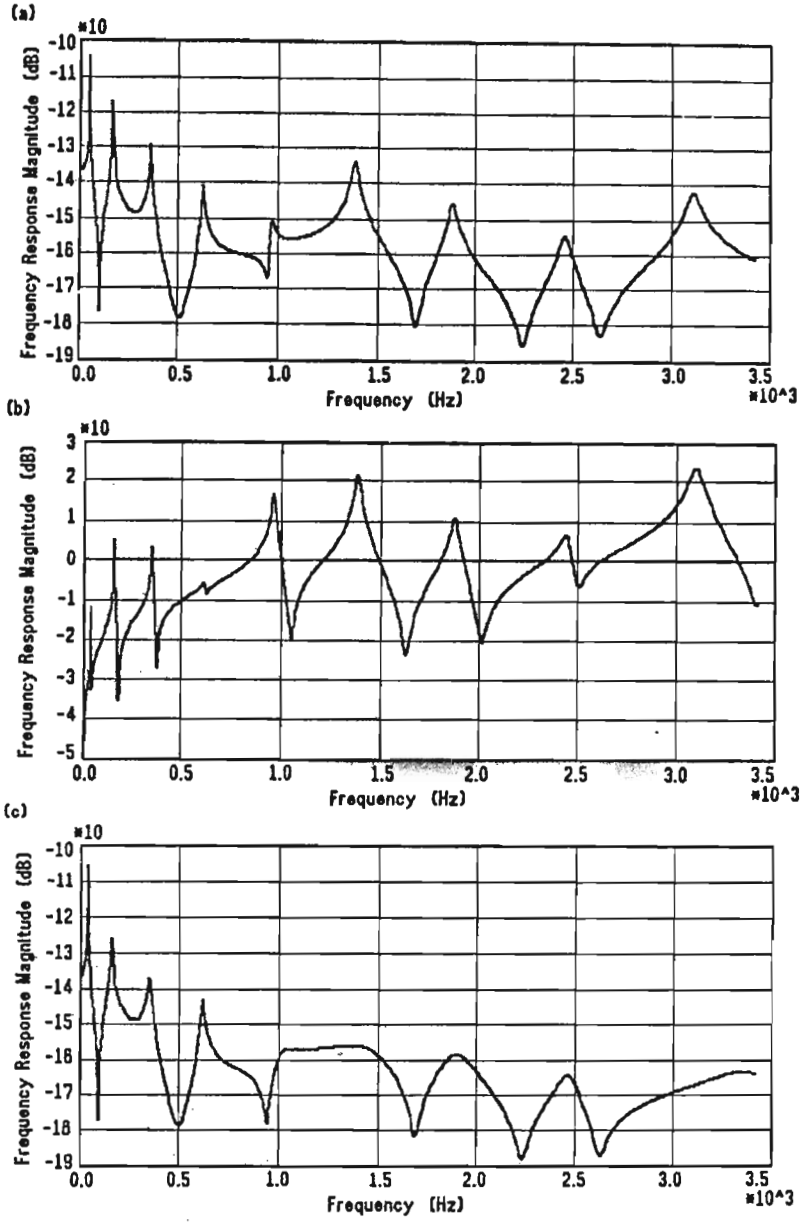

Fig. 5. Frequency response functions for the actuator/sensor location between $x_1 = 0.081$ m and $x_2 = 0.119$ m; (a) magnitude of transfer function G (deflection to voltage input) at $x = 0.15$ m, (b) magnitude of open-loop transfer function G_o (voltage output to voltage input), (c) magnitude of closed-loop transfer function G_c (deflection to voltage input) at $x = 0.15$ m

Hz, ω_5 = 955 Hz, ω_7 = 1870 Hz, ω_9 = 3100 Hz. For the even modes the center line of the actuator lies on the modal line where an inflection point exists. Therefore, as a result of a minimum curvature, the bending moment created by the actuator is negligible. The above explanation concerns the sensing layer. In Fig.4b the magnitude plot of the open-loop transfer function calculated using Eq (6.3) is shown. The output voltage is characterized by a sequence of the odd modes with alternate pole/zero pairs. The resonance peaks become greater for higher frequencies because of the greater curvature of the structure in the region of the actuator. For the closed-control loop with the velocity feedback, the frequency function defined as the ratio of deflection of the structure to the outer input voltage, Eq (6.4), is presented in Fig.4c. The response differs significantly from the plot given in Fig.4a, especially, when the driving frequency lies in the range of resonance. The poles which occur at lower frequencies (ω_1, ω_3) are reduced and they do not exist in higher frequencies $(\omega_5, \omega_7, \omega_9)$. This is the effect of the active damping of the structural vibration.

When the center line of the actuator/sensor electrode and the line of the beam, where deflection is mesured, do not coincide with the modal line, all modes in the frequency response can be observed. The response caused by the outer input voltage calculated at $x = 0.15$ m is characterized by poles that occur at all resonance frequencies in the considered range, Fig.5a. The alternate pole/zero pairs dominate in the plot, however, some pairs of poles appear in sequence, without a zero in between. In the considered case this phenomenon can be noticed between the 2nd and 3rd pole and between the 5th and 6th pole. The magnitude plot of the open-loop transfer function has in general the alternating pole/zero pattern, Fig.5b. The output voltage increases sharply at resonance frequencies except the 4th mode which is characterized by the nodal line laying close to the center line of the sensor. The small curvature of the structure in the sensing region for the 1st mode causes inability of the sensor to induce a high voltage. The output voltage produced in the control loop is fed back to the actuator to obtain the active damping. In Fig.5c the magnitude plot of the closed-loop transfer function is presented. By comparing Fig.5a and Fig.5c, it can be seen that the resonance peaks are reduced. The effect of active damping is greater for the frequencies referring to the high efficiency of the sensor $(\omega_5, \omega_6, \omega_9)$. The magnitude between a pair of poles occurring in sequence changes slightly and still has a considerable value. This kind of response is disadvantageous for the structure dynamic behaviour and occurs because the actuator and sensor signals are not compatible.

The effect of active damping can be illustrated by comparing the deflection distributed along the beam longitudinal axis produced by the actuator voltage input for the system without control loop with this for the system with velocity feedback. Assuming that the actuator/sensor surface electrode is located near the left support, the distributed deflection diagrams calculated at four driving fre-

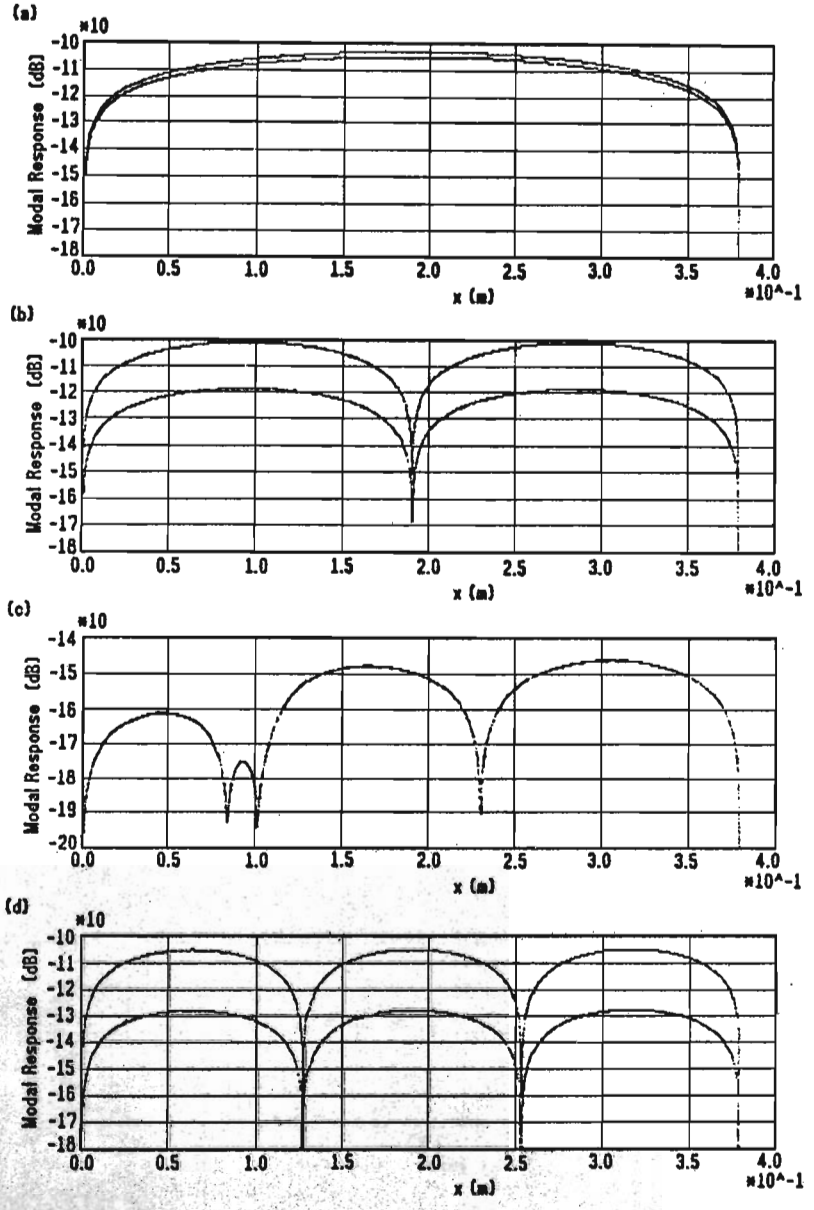

Fig. 6. Beam deflection distribution (a) at 38.2 Hz (at first resonance), (b) at 153 Hz (at second resonance), (c) at 200 Hz (off resonance), (d) at 344 Hz (at third resonance) for the actuator/sensor location: $x_1 = 0.081$ m, $x_2 = 0.119$ m. 1 – the system without control loop, 2 – the system with velocity feedback

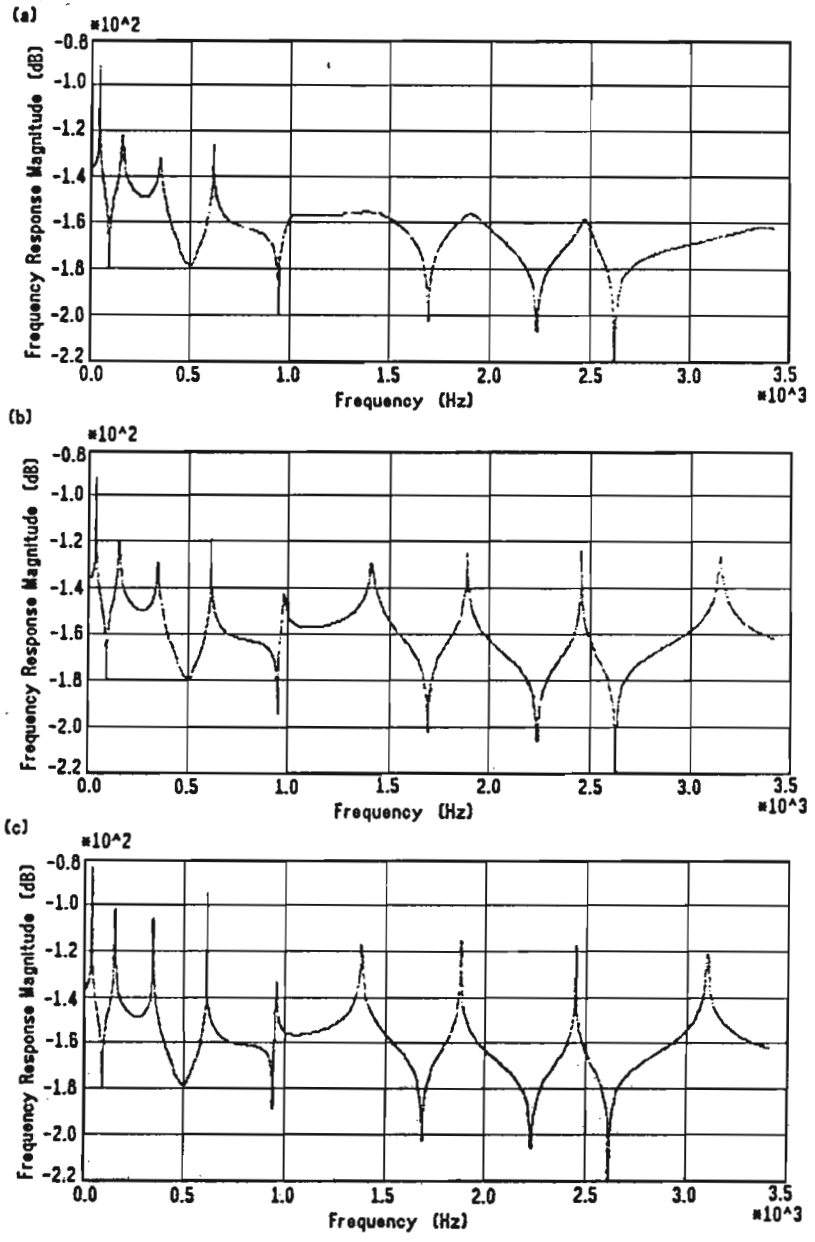

Fig. 7. Closed-loop frequency response functions calculated at $x = 0.15$ m for the differentiator time-lag constant (a) $T = 0.0$ s, (b) $T = 0.0005$ s, (c) $T = 0.01$ s. The actuator/sensor location is: $x_1 = 0.081$ m, $x_2 = 0.119$ m. The nodal damping factor $\gamma = 10^{-6}$

quencies are given in Fig.6. As it was expected, the compared amplitude plots corresponding to the first mode (at 38.2 Hz) differ slighty, Fig.6a, because of the small curvature of the actuating/sensing region. For this reason, the distributed deflection at frequency 200 Hz is nearly the same for both cases, Fig.6c. Here, the driving frequency is off-resonance and belongs to the range between the pair of poles occurring in sequence (see Fig.5). The damping effect is significant at resonance frequencies refering to the second and the third mode as shown in Fig.6b and Fig.6d, respectively. For the above modes the actuator/sensor responds efficiently.

In the considered system the velocity feedback is composed applying the differentiating element characterized by the time-lag constant T. The influence of the value of parameter T on the closed-loop frequency response is presented in Fig.7. To increase the testing effect the small modal damping factor $\gamma = 10^{-6}$ is used in the calculation. By comparing Fig.7a and Fig.7b obtained for the time-lag constant $T = 0.0$ s and $T = 0.0005$ s respectively, the magnitude increment is observed, particularly, at higher resonance frequencies. However, for the large time-lag constant $T = 0.01$ s (see Fig.7c) the resonance peaks differ significantly from those calculated for $T = 0.0$ s even at low frequencies. The phase displacement between the signals from the actuator and sensor induced by the time-lag of the differentiator causes that the actuator/sensor pair does not operate effectively. The presence of damping in real systems diminishes the effect exposed in Fig.7. Since, the time-lag constants of the applied PD-control elements are smaller then 10^{-3} s, so the influence of the phase displacement on the system response can be neglected.

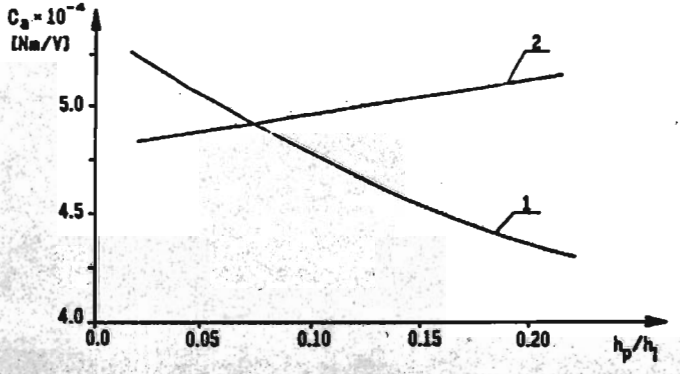

Fig. 8. The actuator constant C_a versus thickness ratio h_p/h_l; 1 – linear stress distribution, 2 – uniform stress distribution in the piezoelectric layer

Fig.8 shows the actuator constant C_a obtained by varying the thickness ratio of the piezoelectric layer and metal strip for the two considered methods of determining the equivalent bending moment. In the first case (line No.1), the linear

stress distribution in the actuator layer and the equivalent bending stiffness of the one-dimensional laminated plate were assumed. It can be seen that the constant C_a declines as the thickness ratio increases. For low thickness ratios, the relationship between the actuator constant as well as the bending moment induced by the actuator is nearly linear. The above results generally agree with those obtained by Wang and Rogers (1991) using the strain-energy model of the mechanical coupling between the actuator and the structure. In the second case (line No.2), the normal stresses in the piezoelectric ply are assumed to be uniform. The actuator constant C_a versus the thickness ratio changes in a different way, i.e., C_a increases in proportion to the increment of the thickness ratio. Inspection of Fig.8 shows that there are stiffness ratios where the both values of the constant C_a are similar $(0.05 < h_p/h_l < 0.1)$. But for law and high thickness ratios, the values of C_a differ significantly. Therefore, the application of the second method to obtain equivalent bending moment is restricted to the narrow range of the stiffness ratio.

8. Conclusions

The theoretical model of a simply supported one-dimensional laminated plate with piezoelectric layers has been studied. To achieve the active damping of the structure, the velocity feedback control is used. The system response is expressed in terms of the transfer functions. The transfer functions for the system with and without control-loop, respectively, have been examined. It was shown that the system response and the sensitivity to generate or damp particular modes depend on the location of the actuator/sensor surface electrode in relation to the modal lines resulting from the boundary conditions.

The phase displacement between the signals from the actuator and sensor caused by the time-lag of the controller can reduce the efficiency of the actuator/sensor pair. However, this effect can be neglected because of damping and a very small value of the time-lag constant in the models of real systems.

Two static models describing the interaction between the actuator and the structure are discussed. It was shown that the simplification of the stress distribution in the piezoelectric layer causes that the bending moment induced by the actuator is underestimated for low and overestimated for high thickness ratios, respectively.

References

1. ALBERTS T.E., COLVIN J.A., 1991, *Transfer function analysis for a flexible beam*

with piezoelectric film actuator and sensor, Proceedings of the Conference on Recent Advances in Active Control of Sound and Vibration, Virginia, 67-77

2. CLARC R.L., FULLER CH.R., WICKS A., 1991, *Characterization of multiple piezoelectric actuators for structural excitation,* J.Acoust.Soc.Am., 90, 346-357
3. CRAWLEY E.F., LUIS J.DE, 1987, *Use of piezoelectric actuators as elements of intelligent structures,* AIAA J., 25, 1373-1385
4. LEE C.-K., CHIANG W.-W., O'SULLIVAN T.C., 1991, *Piezoelectric modal sensor/actuator pairs for critical active damping vibration control,* J.Acoust.Soc.Am., 90, 374-384
5. NEWMAN M.J., 1991, *Distributed active vibration controllers,* Proceedings of the Conference on Recent Advances in Active Control of Sound and Vibration, Virginia, 579-592
6. PAN J., HANSEN C.H., SNYDER S.D., 1991, *A study of the response of a simply supported beam to excitation by a piezoelectric actuator,* Proceedings of the Conference on Recent Advances in Active Control of Sound and Vibration, Virginia, 39-49
7. WANG B.-T., ROGERS C.A., 1991, *Modeling of finite-length spatially-distributed induced strain actuators for laminate beams and plates,* J.of Jntell.Mater.Syst.and Struct., 2, 38-57
8. WHITNEY J.M., 1987, *Structural analysis of laminated anisotropic plates,* Technomic Publishing Co.Inc, Lancaster

Kontrolowanie i redukcja drgań jednowymiarowych piezoelektrycznych laminatów

Streszczenie

W pracy zbadano model swobodnie podpartej trójwarstwowej jednowymiarowej płyty z okleinami piezoelektrycznymi, które stanowią parę wykonawczo-pomiarową. Aktywne tłumienie drgań uzyskano poprzez sprzężenie zwrotne o sygnale proporcjonalnym do prędkości zmian napięcia wytwarzanego przez element pomiarowy.

Wyznaczono przepustowości widmowe odpowiadające stosunkowi ugięć płyty do napięcia zewnętrznego zasilającego element wykonawczy w przypadku układu bez sprzężenia zwrotnego i układu zamkniętego ze sprzężeniem zwrotnym. Określono także przepustowość widmową układu otwartego.

Na podstawie wyników eksperymentu numerycznego pokazano wpływ lokalizacji pary wykonawczo-pomiarowej oraz parametrów sterujących na dynamiczną odpowiedź układu.

Manuscript received September 3, 1992, accepted for print February 26, 1993